

Distinct variation of electronic states due to annealing in T' -type $\text{La}_{1.8}\text{Eu}_{0.2}\text{CuO}_4$ and Nd_2CuO_4 Shun Asano,^{1,2} Kenji Ishii,³ Daiju Matsumura,⁴ Takuya Tsuji,⁴ Kota Kudo,¹ Takanori Taniguchi,² Shin Saito,⁵ Toshiki Sunohara,⁵ Takayuki Kawamata,⁵ Yoji Koike,⁵ and Masaki Fujita^{2,*}¹*Department of Physics, Tohoku University, Aoba, Sendai 980-8578, Japan*²*Institute for Materials Research, Tohoku University, Katahira, Sendai 980-8577, Japan*³*Synchrotron Radiation Research Center, National Institutes for Quantum and Radiological Science and Technology, Hyogo 679-5148, Japan*⁴*Materials Sciences Research Center, Japan Atomic Energy Agency, Hyogo 679-5148, Japan*⁵*Department of Applied Physics, Graduate School of Engineering, Tohoku University, Sendai 980-8579, Japan*

(Received 21 May 2020; revised 7 September 2021; accepted 29 November 2021; published 13 December 2021)

We performed Cu K -edge x-ray absorption fine-structure measurements on T' -type $\text{La}_{1.8}\text{Eu}_{0.2}\text{CuO}_4$ (LECO) and Nd_2CuO_4 (NCO) to investigate the variation in the electronic state associated with the emergence of superconductivity due to annealing. The x-ray absorption near-edge structure spectra of as-sintered (AS) LECO are quite similar to those of AS NCO, indicating that the ground state of AS LECO is a Mott insulator. We clarified a significant variation in the electronic state at the Cu sites in LECO due to annealing. The electron density after annealing n_{AN} was evaluated for both superconducting LECO and nonsuperconducting NCO and was found to be 0.40 and 0.05 electron per Cu atom, respectively. In LECO but not in NCO, extended x-ray absorption fine-structure analysis revealed a reduction in the strength of the Cu-O bond in the CuO_2 plane due to annealing, which is consistent with the screening effect on phonons in the metallic state. Since the amounts of oxygen loss due to annealing δ for LECO and NCO are comparable, these results suggest distinct electron-doping processes in the two compounds. The electron doping in NCO approximately follows the relation $n_{\text{AN}} = 2\delta$; this can be understood if electrons are doped through oxygen deficiency, but the anneal-induced metallic nature and large n_{AN} in LECO suggest that a variation of the electronic band structure causes the self-doping of carriers. The origin of the difference in doping processes due to annealing is discussed in relation to the size of the charge-transfer gap.

DOI: [10.1103/PhysRevB.104.214504](https://doi.org/10.1103/PhysRevB.104.214504)**I. INTRODUCTION**

Single-layer cuprate oxides $R_2\text{CuO}_4$ (where R refers to rare earth) possess three structural isomers. The T' -type isomer has four oxygens coordinated around the Cu ion, the T^* type has five, and the T type has six. Historically, all forms of $R_2\text{CuO}_4$, regardless of their oxygen-coordination numbers, have been assumed to be Mott insulators with a charge-transfer (CT) gap and parent compounds of high-transition-temperature superconductors. However, the reported observation of superconductivity in T' -type $R_2\text{CuO}_4$ has raised the possibility that the ground states of $R_2\text{CuO}_4$ structural isomers are not unique [1–3]; this inaugurated the study of how different oxygen coordinations affect the physical properties of the isomers [4–6].

Thus far, superconductivity in Ce-free (undoped) T' -type $R_2\text{CuO}_4$ has been observed in limited samples such as thin films after adequate oxygen reduction annealing [1]. In the case of single-crystal and high-temperature synthesized powder samples of $R_{2-x}\text{Ce}_x\text{CuO}_4$, grown via the conventional method, superconductivity has not been realized at $x = 0$ even for annealed samples [7–10]. Given that the ground state of T' -type $R_2\text{CuO}_4$ is metallic, the removal of partially existing

excess oxygens at the apical site is the key to achieving superconductivity; this can be realized homogeneously for the thin film because of the large surface-to-volume ratio.

Recent studies on photoemission and soft x-ray absorption spectroscopy have presented evidence of annealing-induced electron doping [10–15]. Based on angle-resolved photoemission spectroscopy experiments on thin-film Pr_2CuO_4 , Horio *et al.* concluded that oxygen nonstoichiometry induced by annealing in the $R_2\text{O}_2$ layer and/or the CuO_2 plane is the origin of such doping [13]. Importantly, this suggests that structural disorder is present even in the superconducting (SC) sample and that the superconductivity in T' -type $R_2\text{CuO}_4$ is the result of electron doping. Thus, it is essential to understand the relationship between the annealing-induced variation of the electronic state and the occupancy (or lack of occupancy) of each site by oxygens. Although reports on the structural information of each oxygen site, i.e., the occupancy and positional parameters of $R_2\text{CuO}_4$, remain limited, neutron diffraction measurements and Rietveld refinement have revealed a similar trend of oxygen structures in the as-sintered (AS) compounds, regardless of R . Annealed (AN) compounds also feature comparable oxygen structures [16–19]. That is, more oxygen defects are present in the $R_2\text{O}_2$ layers than in the CuO_2 plane, and these defects are insensitive to annealing. Partially existing apical oxygens in the AS sample can be removed via annealing.

*fujita@imr.tohoku.ac.jp

There are two possible scenarios for electron doping through annealing:

(i) The first is electron doping into the Cu $3d_{x^2-y^2}$ upper Hubbard band (UHB) by removal of the apical oxygen and/or by induced oxygen deficiency [see Fig. 5(c) below]. In this case, the increased electron density after annealing n_{AN} is given by $n_{AN} = 2\delta$, where δ is the total amount of reduced oxygen in the formula unit due to annealing.

(ii) The second is self-doping associated with the collapse of the CT gap [20–22] [see Fig. 5(d) below]. It has been proposed that the removal of the apical oxygen lowers the Madelung energy of the Cu $3d_{x^2-y^2}$ UHB [21], resulting in the hybridization with the O $2p$ band on the Fermi level. In this situation, both electron and hole carriers could be generated simultaneously.

A recent x-ray absorption near-edge structure (XANES) study on high-temperature synthesized $\text{Pr}_{2-x}\text{Ce}_x\text{CuO}_4$ (PCCO) [23] found that, although $n_{AN} = 2\delta$ in the smaller- δ region, it tends to be higher in the larger- δ region. This result suggests that the sequential electron-doping process (i) leads to the self-doping process (ii) with increasing δ . To understand the mechanism of undoped superconductivity in T' -type $R_2\text{CuO}_4$, it is necessary to clarify how annealing induces electron transfers unseen in the non-SC compound. For this purpose, a powder sample of T' -type SC $\text{La}_{1.8}\text{Eu}_{0.2}\text{CuO}_4$ (LECO) synthesized via a soft chemistry technique would be an excellent candidate system [3]. However, LECO can be obtained only in the form of powder, and therefore, the experimental methods that can be used to evaluate the detailed electronic states are limited.

In this study, we performed Cu K -edge x-ray absorption fine-structure (XAFS) measurements on LECO and high-temperature synthesized Nd_2CuO_4 (NCO). The latter remains non-SC even after annealing. By investigating the XANES spectra of LECO, we clarified a significant evolution of the electronic state at Cu sites due to annealing, with a large n_{AN} value of 0.40 electron per Cu atom. Furthermore, extended x-ray absorption fine-structure (EXAFS) analysis indicated that the strength of the Cu-O bond in the CuO_2 plane (Cu-O_p) was reduced due to annealing, which is consistent with the screening effect on phonons in the metallic state. By contrast, for NCO, n_{AN} and δ were found to be 0.05 electron per Cu atom and 0.035 per formula unit, respectively, approximately following the $n_{AN} = 2\delta$ relation; no evidence of the weakening of the Cu-O_p bond due to annealing was observed. As the δ values of LECO and NCO are comparable, these results suggest that the variation in the electronic state due to annealing proceeds in a different manner in each compound.

II. SAMPLE PREPARATION AND XAFS EXPERIMENT

AS polycrystalline samples of LECO were synthesized using a soft chemistry method, as described in the literature [3]. SC LECO with a transition temperature T_c of 20 K was obtained by annealing the AS samples in vacuum at 700 °C for 24 h. AS polycrystalline samples of NCO were synthesized using the conventional solid-state reaction method. AN NCO was prepared by annealing the AS NCO under flowing Ar gas at 750 °C for 12 h. The phase purity of the samples was checked through x-ray powder diffraction at room tem-

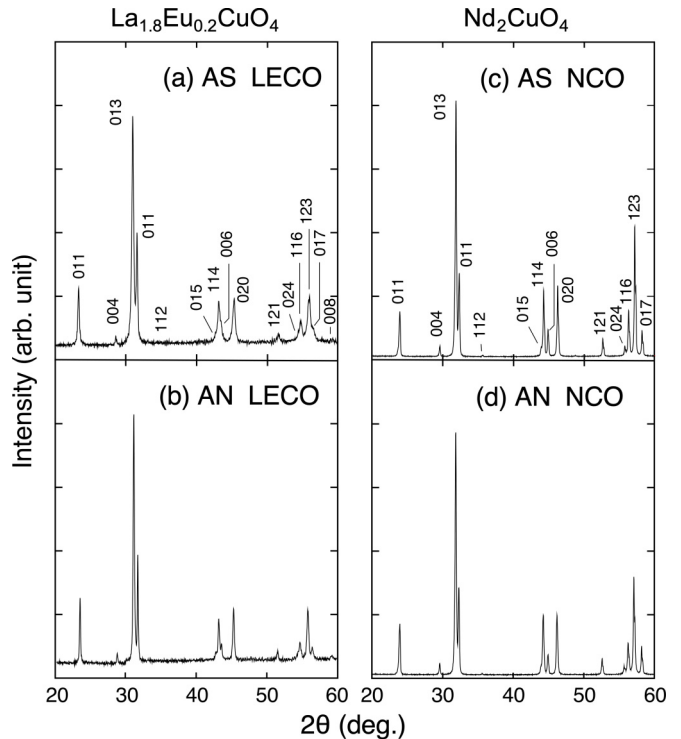


FIG. 1. X-ray diffraction pattern for (a) as-sintered (AS) and (b) annealed (AN) $\text{La}_{1.8}\text{Eu}_{0.2}\text{CuO}_4$ (LECO) and (c) AS and (d) AN Nd_2CuO_4 (NCO).

perature. As shown in Fig. 1, no evidence of the impurity phase was observed for all the samples. The observed Bragg reflections are well indexed for the tetragonal structure with $I4/mmm$ symmetry. Lattice constants evaluated via Rietveld analysis on the x-ray diffraction pattern for LECO and NCO are shown in Table I. In both LECO and NCO, the in-plane (out-of-plane) lattice is slightly elongated (shrunk) due to annealing. For NCO, we determined the value of δ to be 0.035 from the weight loss of the sample through annealing. This δ is the standard value for NCO [24]. Furthermore, our recent neutron diffraction measurements clarified that the structural changes in each oxygen site of LECO due to annealing [19] are similar to those in single-crystal NCO reported previously [16]. The evaluated δ for LECO from the structural analysis is ~ 0.05 , which is approximately the same as that for NCO. According to the neutron diffraction study revealing a similar trend for the oxygen structure in $R_2\text{CuO}_4$ [16–19], the comparable δ values imply no significant difference in the structural change induced by annealing. We therefore believe that the variation in electronic states due to annealing between LECO

TABLE I. Lattice constants for as-sintered (AS) and annealed (AN) compounds of $\text{La}_{1.8}\text{Eu}_{0.2}\text{CuO}_4$ (LECO) and Nd_2CuO_4 (NCO).

	a (Å)	c (Å)
AS LECO	3.9994(7)	12.485(4)
AN LECO	4.0037(2)	12.459(1)
AS NCO	3.9452(5)	12.176(1)
AN NCO	3.9463(5)	12.172(1)

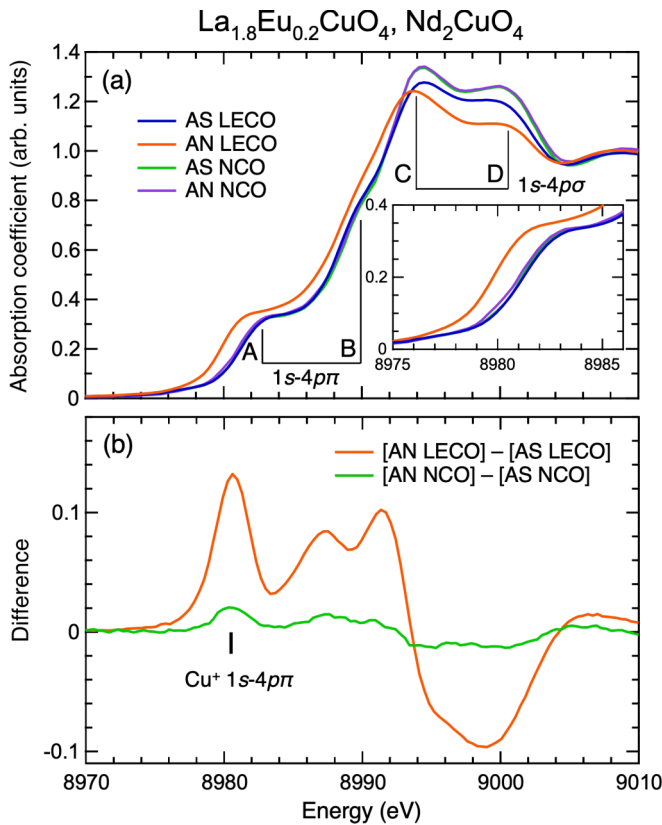


FIG. 2. (a) Cu K -edge XANES spectra for AS and AN LECO. The XANES spectra for AS and AN NCO are plotted as a reference. The inset presents the enlarged spectra for the energy between 8975 and 8986 eV. (b) The difference spectra for LECO and NCO, which are obtained by subtracting the spectra of the AS compounds from those of the AN compounds.

and NCO can be compared in terms of the similar structural changes of the oxygen atoms.

Cu K -edge XAFS measurements were performed with the transmission mode at the BL01B1 and BL14B1 beamlines at the SPring-8 synchrotron radiation facility. Using a Si(111) double-crystal monochromator, we measured the XAFS spectra at 300 K on small pellets (7 mm in diameter and 0.5 mm in thickness), which were mixed with boron nitride for self-support. XAFS spectra consist of XANES and EXAFS spectra, reflecting the unoccupied electronic state and the local structure around the Cu site, respectively. The temperature dependence of the EXAFS spectra was measured from 10 to 300 K to analyze the atomic mean square relative displacement C_2 ($= \sigma_s + \sigma_d$) of the Cu-O_p bond. Here, σ_s (σ_d) is the static (dynamical) displacement component and is attributed to the random displacement of atomic positions (thermal vibration of atoms).

III. RESULTS

Figure 2(a) shows XANES spectra for AS and AN LECO. The spectrum for AS NCO is also plotted in Fig. 2(b) as a reference. The AS samples of LECO and NCO exhibit highly similar spectra, indicating the same electronic state in both

AS compounds. This similarity is consistent with the previous results for AS Pr₂CuO₄ [23]. The small difference in the structure around 8994 and 9000 eV, energies corresponding to the $1s$ - $4p\sigma$ transitions, can be understood by the variation of the size of rare-earth atoms [25]. Therefore, the ground state of AS T' -type R_2 CuO₄ does not depend on the synthesis method. The identification of the same ground state in AS LECO and NCO is an important starting point for discussing the variation of the electronic state in the two compounds due to annealing.

As seen in Fig. 2(a), annealing induces a drastic change in the XANES spectrum of LECO. The intensity around energies corresponding to the $1s$ - $4p\pi$ transitions (8983 and 8991 eV) increases, whereas that around the $1s$ - $4p\sigma$ transitions (8994 and 9000 eV) decreases. A similar spectral change has been observed for PCCO with Ce substitution; this suggests electron doping into the sample [23,25–27].

To clarify the spectral change due to annealing, we subtract the XANES spectrum of AS LECO from that of AN LECO. The difference spectrum of LECO is shown in Fig. 2(b), together with the analogous result for NCO. The amplitude of the difference spectrum is significantly larger for LECO, demonstrating that annealing has a stronger effect on the electronic state. The peak at 8981 eV in the difference spectrum reflects the $1s$ - $4p\pi$ dipole transition of Cu⁺; the existence of a positive intensity therefore indicates the formation of Cu⁺ ($3d^{10}$) sites in the sample due to annealing. By analyzing the intensity, we can evaluate n_{AN} while considering the previous XAFS results of AS PCCO [23,28]. The value of n_{AN} obtained for LECO was 0.40 electron per Cu atom, which is considerably larger than the electron density of 0.21 electron per Cu atom in SC PCCO with $x = 0.16$ [23]. Thus, a large number of electron carriers exist in SC LECO, whereas the number of doped electrons in non-SC NCO due to annealing is rather small ($n_{AN} \sim 0.05$ electron per Cu atom). The latter result is consistent with the recent resonant inelastic x-ray (RIXS) scattering study on NCO reporting that annealing corresponds to a few percent electron doping per Cu atom [29]. Because the δ values of LECO and NCO are comparable, the variation of the electronic state caused by annealing differs between the two compounds. We will discuss the doping process due to annealing for LECO and NCO later.

Next, we analyzed the EXAFS spectra. Since the amount of removed oxygen is significantly small, it can be considered that the change in the XANES spectra reflects only the local information around the removed oxygens. Thus, we examined whether the variation in the electronic state due to annealing occurs throughout the LECO sample, from the structural perspective. Figure 3 shows $|\chi(r)|$, the absolute value of the Fourier transform of the EXAFS oscillations $k\chi(k)$ in the region of $3 \leq k \leq 10 \text{ \AA}^{-1}$ for LECO and NCO. (The results for AS samples are shifted along the vertical direction by 0.4 \AA^{-2} for visual clarity.) In Fig. 3, the Fourier-transform peaks/shoulders corresponding to Cu-O_p, Cu- R ($R = \text{La, Eu, Nd}$), Cu-O_{RE}, and Cu-Cu bonds can be observed. For both LECO and NCO, the overall shape of $|\chi(r)|$ is the same for the AS and AN samples. Thus, the structural change due to annealing is negligible or small. However, at each temperature, the amplitude is smaller for LECO than for NCO, which

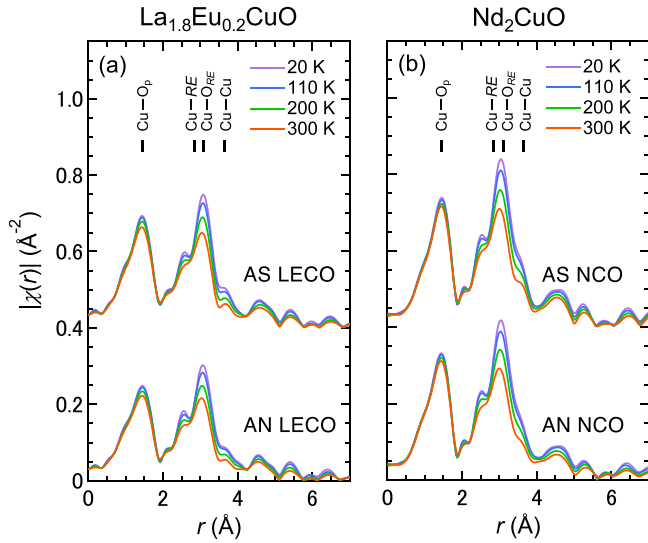


FIG. 3. The absolute value of the Fourier transform of the EXAFS oscillations for (a) AS and AN LECO and (b) AS and AN NCO measured at 20, 110, 200, and 300 K. The solid bars denote the corresponding positions for Cu-O_p, Cu-R ($R = \text{La, Eu, Nd}$), Cu-O_{RE}, and Cu-Cu paths. O_p and O_{RE} represent oxygen sites in the CuO₂ plane and in the R₂O₂ layer, respectively. The results for AS samples are shifted along the vertical direction by 0.4 \AA^{-2} .

implies that considerably more static disorder exists in SC LECO than in non-SC NCO.

The amplitude of each peak/shoulder decreases upon heating due to the thermal vibration of the atoms. The intensity of the peak at $\sim 1.5 \text{ \AA}$ was analyzed to obtain C_2 for the Cu-O_p bond. Figures 4(a) and 4(b) show the temperature dependence of C_2 for LECO and NCO, respectively. To better visualize the different annealing effects on LECO and NCO, C_2 for the AS samples is shifted along the vertical direction. Upon heating, C_2 of AN LECO increases more rapidly than that

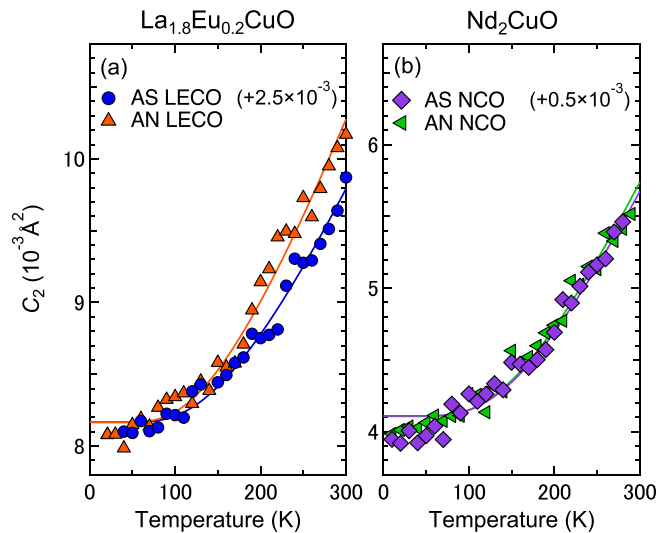


FIG. 4. Temperature dependence of the atomic mean square relative displacement for the Cu-O_p bond C_2 in AS and AN (a) LECO and (b) NCO. The solid lines represent fitting results using Eq. (1).

TABLE II. Energy of Einstein oscillator $\hbar\omega_E$ for AS and AN compounds of LECO and NCO, amplitude of softening due to annealing $\Delta\hbar\omega_E$, and static atomic mean square relative displacement σ_s .

	$\hbar\omega_E$ (meV)	$\Delta\hbar\omega_E$ (meV)	σ_s (10^{-3} \AA^2)
AS LECO	44.3(4)		2.0(1)
AN LECO	40.6(4)	3.7(4)	4.1(1)
AS NCO	44.8(5)		0(1)
AN NCO	44.2(4)	0.6(5)	0.5(1)

of AS LECO. This rapid increase indicates the weakening of the Cu-O_p bond strength due to annealing; this is consistent with the result of the present XAFS; the large number of mobile carriers induced by annealing can screen long-range Coulomb forces on the atomic nuclei. As a result, the effective interaction between neighboring atoms is weakened, and the phonons are softened in the metallic state. The softening of longitudinal optical phonons (corresponding to the Cu-O bond stretching mode) due to electron doping has indeed been observed at around the Γ point in T' -type cuprates [30,31]. Given that the phonons measured via EXAFS exhibit the bulk nature, the phonon softening caused by the screening effect suggests that the entire sample is converted to the metallic state. Therefore, we conclude that the variation in the electronic state due to annealing is a bulk phenomenon that occurs throughout the LECO sample. This conclusion is consistent with the emergence of bulk superconductivity in LECO. By contrast, no clear annealing effect on the thermal evolution of C_2 was observed for NCO, where n_{AN} is rather small.

Based on the Einstein model, the temperature dependence of C_2 was analyzed using the equation

$$C_2 = \sigma_s + (\hbar/2\mu\omega_E)\coth(\hbar\omega_E/2k_B T), \quad (1)$$

where ω_E is the oxygen frequency of Einstein oscillators and μ is the reduced mass of copper and oxygen atoms. Here, \hbar and k_B represent the reduced Planck constant and Boltzmann constant, respectively. For all the samples, we assumed a temperature-independent σ_s since no evidence of structural transitions was observed in the measured temperature range. The values of $\hbar\omega_E$ evaluated for each sample are summarized in Table II. In the AS compounds, the $\hbar\omega_E$ values for LECO and NCO are comparable. However, ω_E for LECO decreases by approximately 10% due to annealing, whereas the annealing effect on ω_E for NCO is negligible. The quantitative analysis further revealed a larger σ_s in AN LECO than in AS LECO, indicating the enhancement of static disorder due to annealing.

IV. DISCUSSION

The present study has demonstrated a drastic variation of the electronic state in LECO associated with the appearance of superconductivity due to annealing. Here, we discuss the possible origin of this variation, as well as the reason that annealing has different effects on the electronic states in LECO and NCO. This discussion focuses on the size of the CT gap.

Mott insulators such as T -type La₂CuO₄ are characterized by the CT gap (with gap energy Δ_{CT}) between the Cu

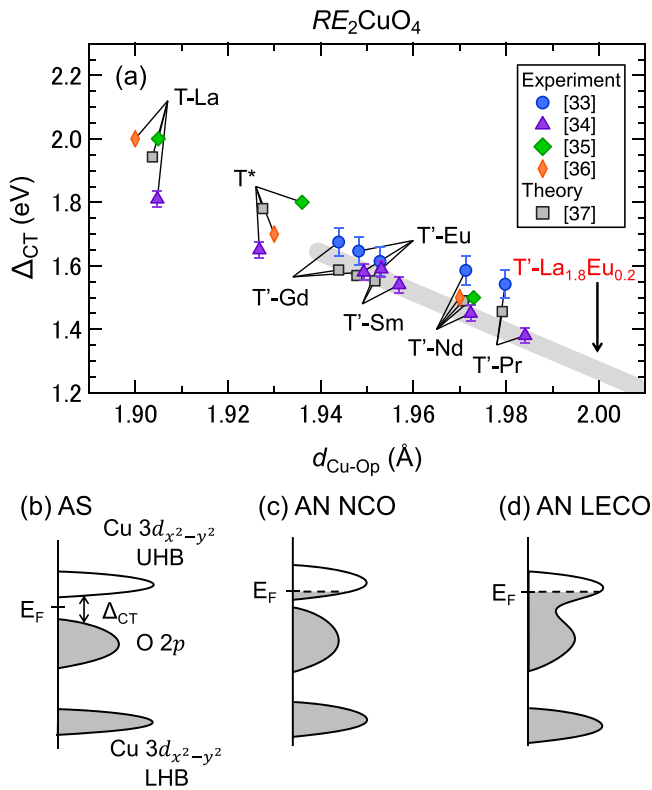


FIG. 5. (a) Energy of the charge-transfer gap Δ_{CT} as a function of the Cu-O_p bond length d_{Cu-O_p} for *T*-type La₂CuO₄ (T-La), *T**-type cuprates (*T**), *T*'-type Pr₂CuO₄ (T'-Pr), *T*'-type Nd₂CuO₄ (T'-Nd), *T*'-type Sm₂CuO₄ (T'-Sm), *T*'-type Eu₂CuO₄ (T'-Eu), *T*'-type Gd₂CuO₄ (T'-Gd), and *T*'-type La_{1.8}Eu_{0.2}CuO₄ (T'-La_{1.8}Eu_{0.2}) [33–36]. All of *T*'-type R₂CuO₄ are AS compounds. Δ_{CT} calculated by the ionic and cluster model is also plotted [37]. The gray solid line acts as a guide. Schematic of the density of states for (b) AS compounds, (c) AN (NCO), and (d) AN LECO.

$3d_{x^2-y^2}$ UHB and the O $2p$ band [32] [Fig. 5(b)]. As a clear gap structure has been observed in the optical conductivity and RIXS spectra of AS NCO [29,33], the similarity in the XANES spectra of AS LECO and AS NCO demonstrates that AS LECO is a Mott insulator. However, the annealing-induced electronic states of the two compounds are quite different, although the structural changes in oxygen ions due to annealing are comparable in the two systems [16,19]. n_{AN} (0.05 electron per Cu atom) and δ (0.035) of NCO approximately follow the $n_{AN} = 2\delta$ relation. This implies that the removal of one oxygen atom predominantly generates two electrons in the system, which is consistent with the electron doping into the UHB without the disappearance of the CT gap, as shown in Fig. 5(c). By contrast, n_{AN} of 0.40 electron per Cu atom for LECO is significantly beyond the expected value from the $n_{AN} = 2\delta$ relation, given that $\delta \sim 0.05$. Thus, numerous electrons exist in the SC sample. As discussed in relation to the previous XANES results for PCCO, the emergence of this large number of electrons indicates the simultaneous generation of holes to maintain charge neutrality. This situation is difficult to explain by a picture based on the electron doping into the UHB with finite Δ_{CT} . In the case of LECO, the

removal of oxygen would cause the collapse of the CT gap, and as a result, both the electrons and holes would emerge at the Fermi level in the hybridized UHB and O $2p$ bands [see Fig. 5(d)]. The collapse of the CT gap may occur on lowering the energy of UHB and/or broadening the bandwidth to reach the O $2p$ band.

We speculate that such a distinct evolution is attributable to the different size of Δ_{CT} in the AS compound. Figure 5(a) shows the Δ_{CT} reported in optical studies [33–36] as a function of the Cu-O_p bond length d_{Cu-O_p} for *T*-, *T**-, and *T*'-type R₂CuO₄. Δ_{CT} , which is correlated with the Madelung energy at the Cu sites, is smaller in the compounds with lower coordination. Furthermore, in *T*'-type R₂CuO₄ with four-coordination, Δ_{CT} decreases with increasing d_{Cu-O} . Since d_{Cu-O_p} for AS LECO corresponding to $a/2$ is 2.00 Å, LECO is expected to have the smallest Δ_{CT} among R₂CuO₄. A CT gap with small Δ_{CT} easily collapses when the in-gap state is filled by a small amount of electron doping and/or when the UHB is lowered by the removal of apical oxygen [21]. Therefore, even though the ground states of LECO and NCO are the same, reduction annealing induces a marked variation of the electronic state in LECO.

Although the AN samples are nonstoichiometric [19], having electrons and chemical defects, and therefore the true ground state of *T*'-type R₂CuO₄ cannot be elucidated, the present study provides an important clue for understanding the undoped superconductivity. According to the results shown in Fig. 5(a), the CT gap potentially closes even in the AS compound with a sufficiently large value of d_{Cu-O_p} , and therefore, the metallic state appears. Combined with the experimental fact that superconductivity is induced with a smaller Ce concentration in *T*'-type R_{2-x}Ce_xCuO₄ with a larger in-plane lattice constant [9,38–40], this implies that undoped superconductivity could be realized in *T*'-type R₂CuO₄. Thus, the ground state of *T*'-type R_{2-x}Ce_xCuO₄ can be controlled by d_{Cu-O_p} . This paves the way for a unified understanding of the physical properties of *T*'-type cuprates from the perspective of the size of Δ_{CT} .

Finally, we discuss the static disorder in *T*'-type R₂CuO₄. In the R₂CuO₄ cuprate oxides, the *T*'-type structure tends to transform into the *T*-type one as the average radius R_{AV} of the rare-earth ion increases [41–45]. This is to alleviate the size mismatch between the Cu-O-Cu and R-R bonds. Our EXAFS measurements revealed a larger value of σ_s in LECO ($R_{AV} = 1.164$ Å) than in NCO ($R_{AV} = 1.123$ Å). This is likely due to LECO's greater structural instability since LECO is located near the phase boundary between *T*' and *T* structures against R_{AV} . In the vicinity of the phase boundary, the elongation of the in-plane lattice constant due to annealing easily enhances the structural instability and increases σ_s , as seen in Table II. Muon spin relaxation measurements suggest the coexistence of short-range magnetic order with superconductivity in the ground state of AN LECO [46]. From the structural perspective, the existence of a magnetic order in SC LECO is attributable to a partial localization of carriers due to the large structural disorder; by contrast, the coexistence of magnetic and SC phases in NCO [47] and Pr_{1-x}LaCe_xCuO₄ [9,48] with a shorter in-plane lattice constant can be discussed from the perspective of macroscopic oxygen inhomogeneities. The structural disorder accompanied by the disorder of the

electrostatic potential causes the localization of carriers, leading to the appearance of static magnetism in the competing SC state. Thus, T_c in LECO could be increased by the suppression of magnetic order through the relaxation of structural disorder.

In summary, reduction annealing effects on the electronic states at Cu sites in LECO and NCO were investigated via Cu K -edge XAFS measurements. The analysis of XANES spectra revealed a significant evolution of the electronic state in LECO due to annealing with a large induced electron density n_{AN} of 0.40 electron per Cu atom. For NCO, the variation is significantly smaller, with n_{AN} of only 0.05 electron per Cu atom. The EXAFS analysis revealed evidence of phonon softening of the Cu-O bond in the CuO_2 plane due to annealing for LECO but not for NCO. Therefore, the electronic states for the two compounds vary by distinct processes, although δ , the amount of oxygen loss due to annealing, is comparable for the two systems. The distinct evolution of the electronic states for LECO and NCO can be attributed to the difference in size of the CT gap in the AS compounds; the electronic

state in LECO, which has a smaller Δ_{CT} , is more sensitive to the oxygen removal that could introduce the electron doping and/or variation in the band structure.

ACKNOWLEDGMENTS

We thank Y. Kimura for the support in the analysis of XAFS data. The synchrotron radiation experiments were performed at BL01B1 and BL14B1 of SPring-8 with the approval of the Japan Synchrotron Radiation Research Institute (JASRI; Proposals No. 2016A1603, No. 2017B3611, and No. 2018B3657). This work was partially performed under the GIMRT Program of the Institute for Materials Research, Tohoku University (Proposals No. 19K0035, No. 20N0001, and No. 202012-CNKXX-0012), and financially supported by KAKENHI (Grants No. 16H02125, No. 16H04004), No. 17K14148, No. 17H02915, and No. 21H04448) from Ministry of Education, Culture, Sports, Science, and Technology (MEXT), Japan.

-
- [1] O. Matsumoto, A. Utsuki, A. Tsukada, H. Yamamoto, T. Manabe, and M. Naito, *Phys. C (Amsterdam, Neth.)* **469**, 924 (2009).
- [2] S. Asai, S. Ueda, and M. Naito, *Phys. C (Amsterdam, Neth.)* **471**, 682 (2011).
- [3] T. Takamatsu, M. Kato, T. Noji, and Y. Koike, *Appl. Phys. Express* **5**, 073101 (2012).
- [4] H. Das and T. Saha-Dasgupta, *Phys. Rev. B* **79**, 134522 (2009).
- [5] C. Weber, K. Haule, and G. Kotliar, *Nat. Phys.* **6**, 574 (2010).
- [6] C. Weber, K. Haule, and G. Kotliar, *Phys. Rev. B* **82**, 125107 (2010).
- [7] H. Takagi, S. Uchida, and Y. Tokura, *Phys. Rev. Lett.* **62**, 1197 (1989).
- [8] M. Brinkmann, T. Rex, H. Bach, and K. Westerholt, *Phys. Rev. Lett.* **74**, 4927 (1995).
- [9] M. Fujita, T. Kubo, S. Kuroshima, T. Uefuji, K. Kawashima, K. Yamada, I. Watanabe, and K. Nagamine, *Phys. Rev. B* **67**, 014514 (2003).
- [10] M. Horio, T. Adachi, Y. Mori, A. Takahashi, T. Yoshida, H. Suzuki, K. Okazaki, K. Ono, H. Kumigashira, M. Arita, H. Namatame, M. Taniguchi, D. Ootsuki, M. Takahashi, T. Mizokawa, Y. Koike, and A. Fujimori, *Nat. Commun.* **7**, 10567 (2015).
- [11] H. I. Wei, C. Adamo, E. A. Nowadnick, E. B. Lochocki, S. Chatterjee, J. P. Ruf, M. R. Beasley, D. G. Schlom, and K. M. Shen, *Phys. Rev. Lett.* **117**, 147002 (2016).
- [12] D. Song, G. Han, W. Kyung, J. Seo, S. Cho, B. S. Kim, M. Arita, K. Shimada, H. Namatame, M. Taniguchi, Y. Yoshida, H. Eisaki, S. R. Park, and C. Kim, *Phys. Rev. Lett.* **118**, 137001 (2017).
- [13] M. Horio, Y. Krockenberger, K. Koshiishi, S. Nakata, K. Hagiwara, M. Kobayashi, K. Horiba, H. Kumigashira, H. Irie, H. Yamamoto, and A. Fujimori, *Phys. Rev. B* **98**, 020505(R) (2018).
- [14] M. Horio, Y. Krockenberger, K. Yamamoto, Y. Yokoyama, K. Takubo, Y. Hirata, S. Sakamoto, K. Koshiishi, A. Yasui, E. Ikenaga, S. Shin, H. Yamamoto, H. Wadati, and A. Fujimori, *Phys. Rev. Lett.* **120**, 257001 (2018).
- [15] M. Horio and A. Fujimori, *J. Phys.: Condens. Matter* **30**, 503001 (2018).
- [16] P. G. Radaelli, J. D. Jorgensen, A. J. Schultz, J. L. Peng, and R. L. Greene, *Phys. Rev. B* **49**, 15322 (1994).
- [17] R. Hord, H. Luetkens, G. Pascua, A. Buckow, K. Hofmann, Y. Krockenberger, J. Kurian, H. Maeter, H.-H. Klauss, V. Pomjakushin, A. Suter, B. Albert, and L. Alff, *Phys. Rev. B* **82**, 180508(R) (2010).
- [18] R. Hord, G. Pascua, K. Hofmann, G. Cordier, J. Kurian, H. Luetkens, V. Pomjakushin, M. Reehuis, B. Albert, and L. Alff, *Supercond. Sci. Technol.* **26**, 105026 (2013).
- [19] M. Fujita, T. Taniguchi, T. Wang, S. Torii, T. Kamiyama, K. Ohashi, T. Kawamata, T. Takamatsu, T. Adachi, M. Kato, and Y. Koike, *J. Phys. Soc. Jpn.* **90**, 105002 (2021).
- [20] H. Yokoyama, M. Ogata, and Y. Tanaka, *J. Phys. Soc. Jpn.* **75**, 114706 (2006).
- [21] T. Adachi, Y. Mori, A. Takahashi, M. Kato, T. Nishizaki, T. Sasaki, N. Kobayashi, and Y. Koike, *J. Phys. Soc. Jpn.* **82**, 063713 (2013).
- [22] K. Yamazaki, T. Yoshioka, H. Tsuchiura, and M. Ogata, *J. Phys.: Conf. Ser.* **871**, 012009 (2017).
- [23] S. Asano, K. Ishii, D. Matsumura, T. Tsuji, T. Ina, K. M. Suzuki, and M. Fujita, *J. Phys. Soc. Jpn.* **87**, 094710 (2018).
- [24] K. Kurahashi, H. Matsushita, M. Fujita, and K. Yamada, *J. Phys. Soc. Jpn.* **71**, 910 (2002).
- [25] G. Liang, Y. Guo, D. Badresingh, W. Xu, Y. Tang, M. Croft, J. Chen, A. Sahiner, B.-H. O, and J. T. Markert, *Phys. Rev. B* **51**, 1258 (1995).
- [26] H. Oyanagi, Y. Yokoyama, H. Yamaguchi, Y. Kuwahara, T. Katayama, and Y. Nishihara, *Phys. Rev. B* **42**, 10136 (1990).
- [27] N. Kosugi, Y. Tokura, H. Takagi, and S. Uchida, *Phys. Rev. B* **41**, 131 (1990).
- [28] S. Asano, K. M. Suzuki, D. Matsumura, K. Ishii, T. Ina, and M. Fujita, *J. Phys.: Conf. Ser.* **969**, 012051 (2018).

- [29] K. Ishii, S. Asano, M. Ashida, M. Fujita, B. Yu, M. Greven, J. Okamoto, D.-J. Huang, and J. Mizuki, *Phys. Rev. Mater.* **5**, 024803 (2021).
- [30] M. d'Astuto, P. K. Mang, P. Giura, A. Shukla, P. Ghigna, A. Mirone, M. Braden, M. Greven, M. Krisch, and F. Sette, *Phys. Rev. Lett.* **88**, 167002 (2002).
- [31] M. Braden, L. Pintschovius, T. Uefuji, and K. Yamada, *Phys. Rev. B* **72**, 184517 (2005).
- [32] J. Zaanen, G. A. Sawatzky, and J. W. Allen, *Phys. Rev. Lett.* **55**, 418 (1985).
- [33] T. Arima, T. Kikuchi, M. Kasuya, S. Koshihara, Y. Tokura, T. Ido, and S. Uchida, *Phys. Rev. B* **44**, 917 (1991).
- [34] S. L. Cooper, G. A. Thomas, A. J. Millis, P. E. Sulewski, J. Orenstein, D. H. Rapkine, S.-W. Cheong, and P. L. Trevor, *Phys. Rev. B* **42**, 10785 (1990).
- [35] Y. Tokura, S. Koshihara, T. Arima, H. Takagi, S. Ishibashi, T. Ido, and S. Uchida, *Phys. Rev. B* **41**, 11657 (1990).
- [36] S. Tajima, S. Uchida, S. Ishibashi, T. Ido, H. Takagi, T. Arima, and Y. Tokura, *Phys. C (Amsterdam, Neth.)* **168**, 117 (1990).
- [37] Y. Ohta, T. Tohyama, and S. Maekawa, *Phys. Rev. Lett.* **66**, 1228 (1991).
- [38] M. Naito, S. Karimoto, and A. Tsukada, *Supercond. Sci. Technol.* **15**, 1663 (2002).
- [39] Y. Krockenberger, J. Kurian, A. Winkler, A. Tsukada, M. Naito, and L. Alff, *Phys. Rev. B* **77**, 060505(R) (2008).
- [40] Y. Krockenberger, B. Eleazer, H. Irie, and H. Yamamoto, *J. Phys. Soc. Jpn.* **83**, 114602 (2014).
- [41] G. Xiao, M. Z. Cieplak, and C. L. Chien, *Phys. Rev. B* **40**, 4538 (1989).
- [42] M. Chaudhri, K. B. Modi, K. Jadhav, and G. Bichile, *Pramana* **48**, 883 (1997).
- [43] Y. Ikeda, K. Yamada, Y. Kusano, and J. Takada, *Phys. C (Amsterdam, Neth.)* **378–381**, 395 (2002).
- [44] C. Zhang and Y. Zhang, *J. Phys.: Condens. Matter* **14**, 7383 (2002).
- [45] Y. Imai, M. Kato, Y. Takarabe, T. Noji, T. Adachi, and Y. Koike, *Phys. C (Amsterdam, Neth.)* **460**, 395 (2007).
- [46] T. Adachi, A. Takahashi, K. M. Suzuki, M. A. Baqiya, T. Konno, T. Takamatsu, M. Kato, I. Watanabe, A. Koda, M. Miyazaki, R. Kadono, and Y. Koike, *J. Phys. Soc. Jpn.* **85**, 114716 (2016).
- [47] E. M. Motoyama, G. Yu, I. M. Vishik, O. P. Vajk, P. K. Mang, and M. Greven, *Nature (London)* **445**, 186 (2007).
- [48] P. Dai, H. J. Kang, H. A. Mook, M. Matsuura, J. W. Lynn, Y. Kurita, S. Komiyama, and Y. Ando, *Phys. Rev. B* **71**, 100502(R) (2005).